

Original Article

DOI 10.1007/s12206-021-0708-8

Keywords:

- Raster angle
- Surface roughness
- Tensile properties
- 3D printing

Correspondence to:Betül Gülçimen Çakan
bgulcimen@uludag.edu.tr**Citation:**

Çakan, B. G. (2021). Effects of raster angle on tensile and surface roughness properties of various FDM filaments. *Journal of Mechanical Science and Technology* 35 (8) (2021) 3347–3353. <http://doi.org/10.1007/s12206-021-0708-8>

Received October 8th, 2020

Revised April 26th, 2021

Accepted May 2nd, 2021

† Recommended by Editor
Chongdu Cho

Effects of raster angle on tensile and surface roughness properties of various FDM filaments

Betül Gülçimen Çakan

Department of Mechanical Engineering, Bursa Uludağ University, Görükle, 16059 Bursa, Turkey

Abstract Parts produced by FDM (fused deposition modelling) technique, where polymer filaments are used, are anisotropic and their properties vary depending on the printing parameters, one of which is raster angle. In this study, the effects of this parameter on the tensile and the surface roughness properties were investigated. It was determined that the ultimate tensile strength (UTS) decreased with increasing raster angle; hence, 0° raster angle where tensile loading direction is parallel to the raster yielded the highest strength. Besides ±45° raster angle resulted the most ductile behaviour with the highest fracture strains. Fracture occurred due to raster failure for 0° raster angle but for 90° raster angle, it was due to the failure of the interlayer raster bonds. In the case of ±45°, both of the failure mechanisms were effective. Surface roughness values increased up to 7 µm when measurement was perpendicular to the raster and dropped below 1 µm when it was parallel to the raster.

1. Introduction

Fused deposition modeling (FDM®) is a 3D printing process which is defined in ASTM Standard Terminology for Additive Manufacturing as “a material extrusion process used to make thermoplastic parts through heated extrusion and deposition of materials layer by layer” [1]. This technique has been favored greatly and found many application fields in a couple of decades. Today, FDM technology is at an affordable cost which made it possible to reach a high number of users in a short span of time. Thanks to their low prices, it has become possible to see FDM printers in schools, homes, many other small and large organizations. Currently, FDM printers have diverse applications e.g. producing prototypes, 3D models for educational purposes or anatomical parts for surgical planning or training and so on [2, 3].

3D printing owes this popularity to its advantages over to conventional production techniques. The most important one is the flexibility in design which enables changing the design of complex parts, which is much more time consuming and costly in conventional techniques. Another advantage is the minimization of the waste or even causing no waste. Possibility of using recycled filaments have also taken attraction due to environmental and cost considerations [4, 5].

As the interest for FDM technology is growing rapidly, producing structural parts with intended mechanical properties rather than parts only serving visual purposes has become a need. A current example is the employment of 3D printing to produce face shields, masks or parts of respiratory equipment to fight against Covid-19 pandemic [6]. This example clearly showed that in situations which requires responding rapidly, 3D printing could be of vital importance. The mechanical properties of the filaments used in FDM process directly affect the mechanical properties of the printed parts. The printed parts exhibit anisotropy and the mechanical properties vary according to the basic printing parameters:

- Building orientation (see Fig. 1);
- Raster angle/orientation (see Fig. 1);
- Layer thickness;
- Infill percentage.

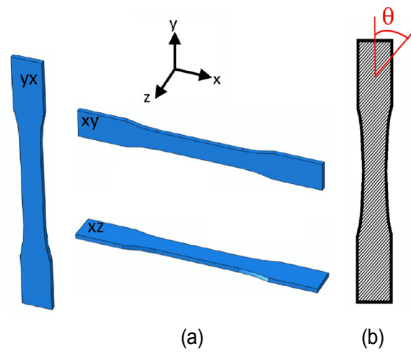


Fig. 1. Printing parameters: (a) building orientation : yx (upright), xy (on-edge), xz (flat); (b) raster orientation/angle (θ).

Therefore, using printed samples to determine the mechanical properties will give more realistic results. In order to evaluate the effects of the above-mentioned printing parameters on mechanical properties, most of the researchers conducted tensile and bending tests [7-9] where for tensile testing, ASTM D638 and ISO 527 standards were preferred [10, 11].

ABS (acrylonitrile butadiene styrene) and PLA (polylactic acid) are the most common filaments used in 3D printing; consequently, they have taken the most attention in the literature. Although not as common, mechanical properties of PEI, PEEK, PC (polycarbonate), PA (polyamide) and some other filaments were also determined in some studies [7]. It is pointed out that as layer thickness decreases/infill percentage increases, ultimate tensile strength (UTS) improves. However, this would bring higher production time and cost.

While there is a common conclusion in literature concerning the effects of layer thickness and infill percentage on tensile properties, different experimental results exist for raster angle. Es-Said et al. and Lanzotti et al. determined that UTS decreased as raster orientation increased, respectively, for PLA and ABS [12, 13]. However, Lecther identified 45° raster orientation as the strongest for PLA filament. In another study, he observed that 0° raster angle yielded the highest mechanical strength compared to 45° and 90° when ABS filament was used [14, 15]. Durgun et al. also investigated the effect of raster orientation with respect to building orientation for ABS filament [16]. Their study showed that 0° raster angle revealed optimum mechanical properties for flat and on-edge building orientations, but upright orientation exhibited inconsistent results compared to those of the other two building orientations. Contrary to all these results, Hernandez et al. concluded that altering the raster orientation resulted in no significant difference in tensile strength of ABS [17].

Due to the variation in results, this study aimed to determine the effect of raster angle on tensile mechanical properties; i.e., UTS, strain at fracture, elastic module by using four different filaments. In addition to the largely used filaments ABS and PLA, two other commercial filaments with the commercial names STH and power ABS were investigated. The obtained results were also compared with the values reported by the

Table 1. Printing parameters.

Parameters	
Layer thickness	0.3 mm
Extrusion width	0.5 mm
Nozzle diameter	0.4 mm
Printing speed	50 mm/s

Table 2. Printing temperatures and filament densities.

	Density [g/cm ³]	Nozzle temperature [°C]	Bed temperature [°C]
ABS	1.100	250	80
PLA	1.240	190	55
POWER ABS	1.032	225	75
STH	1.220	195	70

suppliers of the filaments for 0° raster angle. Lastly, fracture patterns and sections were presented and evaluated considering the tensile test results. Also, surface roughness measurements were carried out for each sample in two directions, i.e. parallel and perpendicular to the tensile loading direction.

2. Materials and methods

In this study, ASTM D638 guidelines were followed for tensile tests [10]. Specimens were flat and had dog bone geometry with the dimensions in Fig. 2, where experimental set-up and a schematic for raster angles are also depicted. Tensile test samples were printed at three different raster angles, namely, 0°, ±45°, 90°, using the xz (flat) building orientation. For each angle, three samples were produced using the printing parameters in Tables 1 and 2. Tensile tests were carried out at a displacement rate of 5 mm/min at ambient temperature by a WDW 100 electronic universal testing machine. The strain rate test samples were subjected to was 1.7x10⁻³ s⁻¹. A hand-held digital microscope was utilized to observe the fracture patterns and sections of the failed samples.

Besides the most widely used filaments ABS (acrylonitrile butadiene styrene) and PLA (polylactic acid), two other commercial filaments, that is, STH and power ABS were investigated [18-20]. These two filaments are reported to have improved properties such as higher impact and heat resistance compared to ABS and PLA. Similar to PLA, STH is also a vegetable-based filament yet its chemical specification is not reported by its supplier. The chemical composition of the power ABS is very similar to traditional ABS basically because it is produced by adding a third material to ABS to enhance the ductility properties. Likewise, this material is not revealed by its supplier.

Surface roughness measurements were performed by portable Time TR200 device according to the ISO standard. Arithmetic average of the roughness, R_a , values were recorded for directions parallel and perpendicular to tensile test direction.

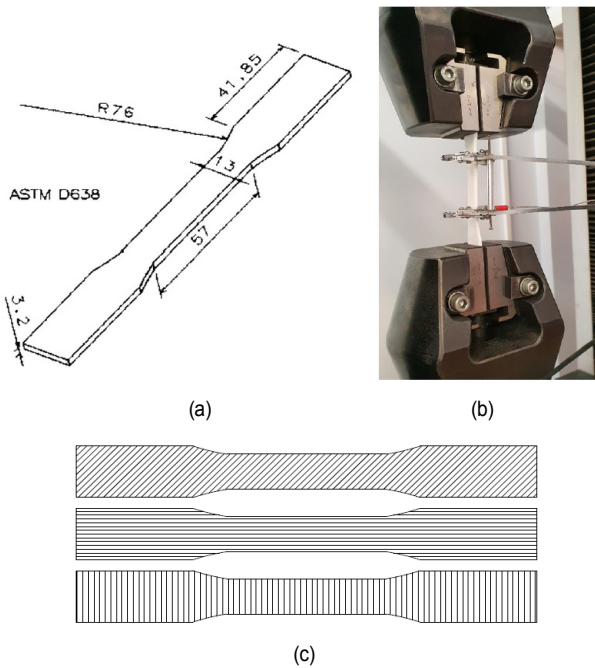


Fig. 2. Tensile test specimen schematic: (a) dimensions according to ASTM D638 with units in mm; (b) the experimental setup; (c) raster angles.

Three measurements were recorded for each sample and average value was calculated.

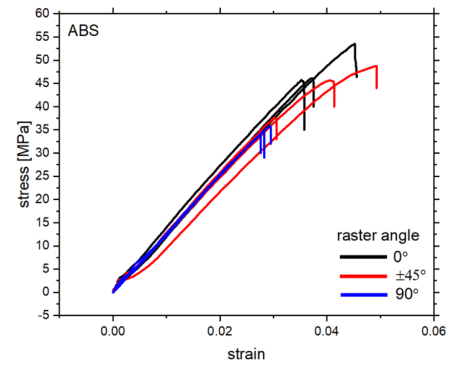
3. Results and discussion

3.1 Tensile test results

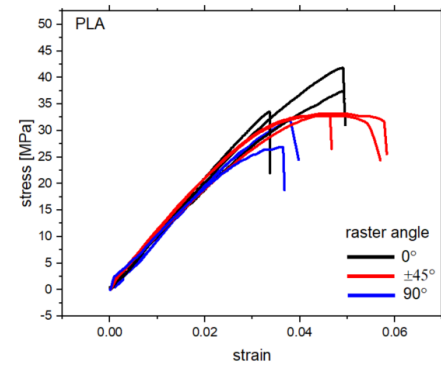
In Figs. 3(a)-(d) engineering stress-strain curves of each filament for 0° , $\pm 45^\circ$, 90° raster orientations are presented. While the curves of ABS and PLA exhibited more brittle nature with instant stress drops following a maximum stress, STH and particularly power ABS revealed necking for most of the samples. All curves were used for determining the average values of the mechanical properties: UTS, fracture strain and elastic module.

The average values for UTS, fracture strain and elastic module for all filaments are plotted with respect to raster orientation in Figs. 4(a)-(c). 0° raster orientation exhibited the highest UTS for all filaments and it consistently decreased with increasing angle. The reason is that for 0° , the filament itself endures the tensile load but as the raster orientation changes from 0° to 90° , the bond strength, which is weaker, plays role in the overall strength. Lanzotti et al. [13] also observed a consistent decrease in UTS values for intermediate raster angle values for PLA filament, which is in agreement with this study.

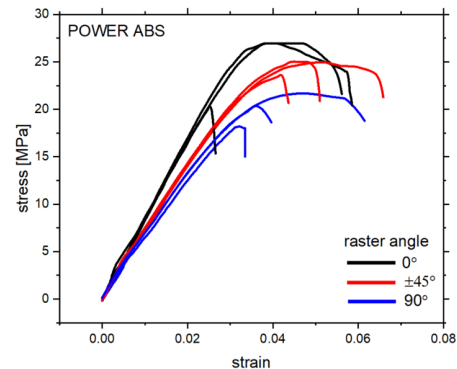
As for fracture strains, $\pm 45^\circ$ raster angle noticeably outperformed the other raster angles for all filaments. Just for ABS filament which acted the most brittle, 0° raster angle's fracture strain was close to that of $\pm 45^\circ$'s. Not as significant as UTS and fracture strain, but elastic modules had also some variation according to raster angle. It may be concluded that 0° raster



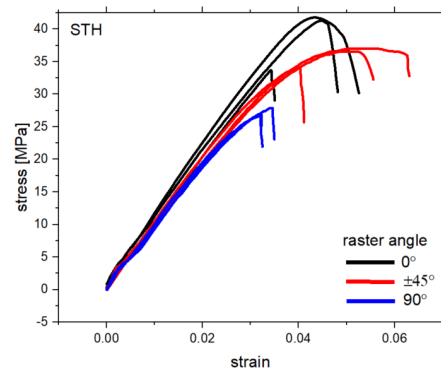
(a)



(b)



(c)



(d)

Fig. 3. Stress-strain curves for ABS, PLA, Power ABS and STH with respect to raster angles 0° , $\pm 45^\circ$, 90° .

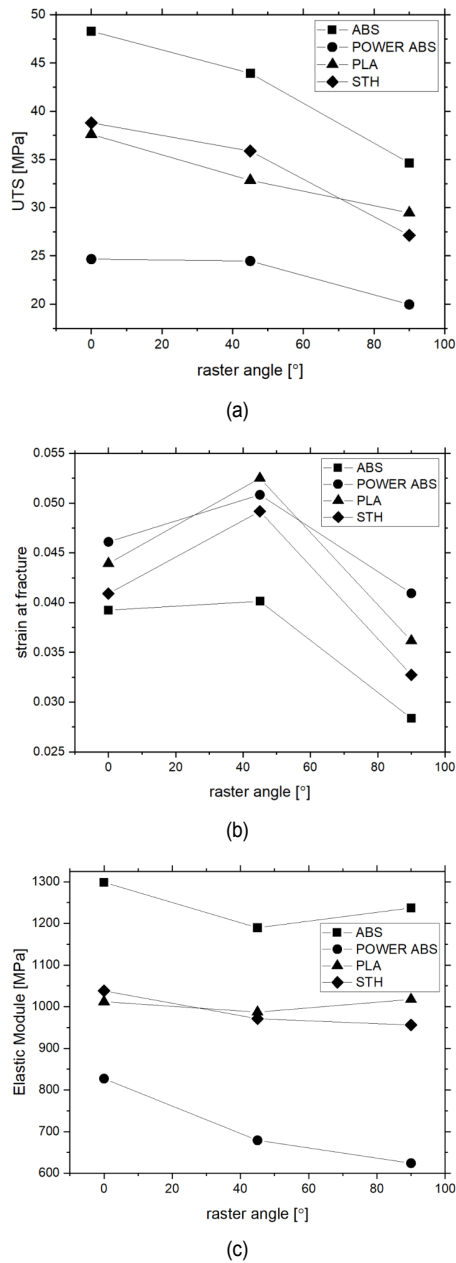


Fig. 4. UTS, Strain at fracture and elastic modules with respect to raster angles 0°, ±45°, 90°.

angle exhibited higher elastic modules. Nevertheless, later it will be shown that this has been the parameter with the highest deviation between the experimental and reported values from the suppliers.

As regards filament comparison, ABS had the highest UTS values but it behaved more brittle compared to other filaments exhibiting lower strain at fracture values. Power ABS was the weakest filament with the lowest UTS but when it comes to ductility, it had a better overall strain at fracture values (considering all raster angles) compared to those of the other filaments. If all mechanical properties are considered, it can be concluded that PLA was found to be favourable with optimized values.

Table 3. Mechanical properties of the filaments provided by their suppliers with the percentage differences from this study's results.

	ABS	PLA	Power ABS	STH
Standard, test rate [mm/min], infill percentage	ISO527, 50, 90 %	ISO527, 50, 90 %	ASTMD638, 2, 100 %	ASTMD638, 50, 100 %
UTS [MPa]	39.0	49.5	10.4	40.7
Strain at fracture [%]	4.8	5.2	na	na
Elastic module [MPa]	1671.5	2346.5	800	4100
% difference for UTS	24	24	137	5
% difference for strain at fracture	18	16	-	-
% difference for elastic module	23	57	3	75

In Table 3, mechanical properties of the filaments provided by their suppliers are listed with the corresponding differences from this study's results. ISO 527 and ASTM D638 test standards were applied by the suppliers using 90 % and 100 % infilled samples. It should be recalled that in this study, 100 % infilled samples were subjected to tensile testing at a rate of 5 mm/min.

The differences between UTS values were minimal for STH filament while for PLA and ABS, the difference increased to 24 %. UTS determined for power ABS was more than the double of the supplier's value though the 100 % infill percentage was used for both. Strain at fracture values were only reported for PLA and ABS which were found to be in agreement with the current results exhibiting 16-18 % differences. Elastic module values showed some inconsistency that may depend on other printing factors which would affect bonding strength. Another possible reason for the significant variations in the material properties between the provided data by the supplier and the experiments could be high the sensitivity of the polymer filaments' physical and mechanical properties to the waiting period after their production.

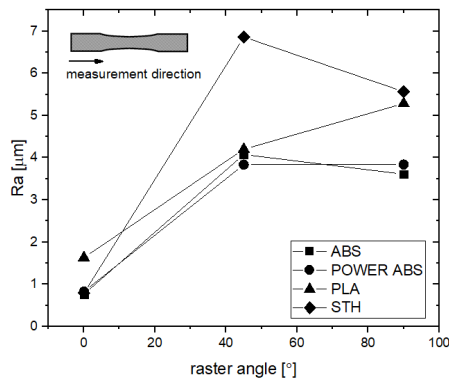
As mentioned before, tensile test samples were produced by 3D printing so as to reflect the mechanical properties of the printed parts. Table 4 presents the percentage differences in mechanical properties for tests carried out for the printed and the molded samples of ABS. Both the UTS and elastic module values are close, while the test data for the molded parts indicates a much higher ductility, thus a much higher strain at fracture value.

3.2 Surface roughness results

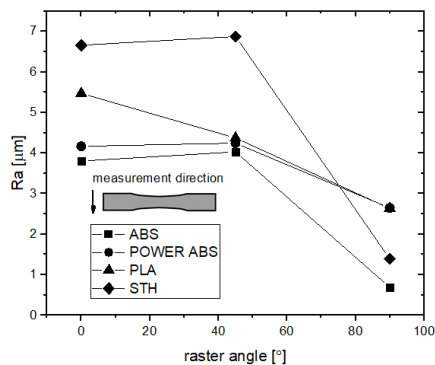
Good surface quality is important in all manufacturing methods in terms of friction, wear and mechanical integrity (i.e., crack forming). The mentioned aspects as well as visibility of

Table 4. Mechanical properties of the ABS filament obtained by ISO 527 tensile tests for the injection molded samples and the percentage differences between the values of the molded and the printed samples.

UTS [MPa]	43.6
Strain at fracture [%]	34
Elastic module [MPa]	2030
% difference for UTS	11
% difference for strain at fracture	86
% difference for elastic module	17



(a)



(b)

Fig. 5. Surface roughness, R_a values with respect to raster angles 0° , $\pm 45^\circ$, 90° taken in two directions: (a) parallel; (b) perpendicular to the tensile loading.

the finished surface are of significance in 3D printing. However, high surface roughness is a drawback in 3D printing compared to traditional methods. The surface quality in 3D printing varies significantly due to the printing parameters; thus, it is important to identify the critical printing parameters which influence it.

Surface roughness results consist of R_a values taken in directions parallel and perpendicular to the tensile loading. All filaments exhibited lower R_a values for 0° raster angle when measurement direction was parallel to the tensile loading, since the measurement was also parallel to the raster for this case (see Fig. 5(a)). Confirming this result, when the measurement was carried out in the perpendicular direction, the measurement direction was parallel to the raster for raster an-

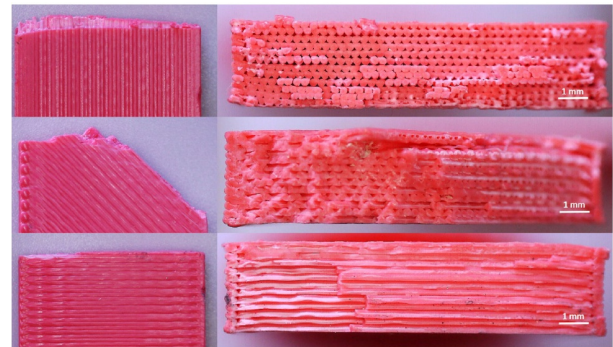


Fig. 6. Fracture patterns (paths) (left) and sections (right) for raster angles 0° (top), $\pm 45^\circ$ (middle), 90° (bottom) for STH filament.

gle of 90° ; consequently, lowest values were obtained for this raster angle (see Fig. 5(b)).

In general, R_a increased up to $7 \mu\text{m}$ for the highest and dropped below $1 \mu\text{m}$ for the lowest cases. While STH exhibited the highest surface roughness values in most of the cases, the values for ABS and power ABS were found to be closer and lower than both STH and PLA.

3.3 Fracture patterns

Representative fracture paths and sections for all filaments are given in Fig. 6 which were taken from STH filament results. Despite the fact that samples were printed with 100 % infill percentage and proper printing parameters to ensure minimum overlap of rasters, some interlayer porosity was noticed in the sections, which could be due to shrinkage of the polymer layers during solidification. This could be possibly improved by adjusting the parameters in Table 1.

In all cases, the fracture initiated from the edge and propagated till a complete fracture occurred. For 0° raster angle, the crack propagated in transverse direction to the applied load and fracture happened due to raster failure.

As for 90° raster angle, the fracture path was also transverse to the applied load but this time, fracture occurred between the interlayer bonds.

The fracture of $\pm 45^\circ$ printed sample comprised the failures of both raster and interlayer bonds with the path starting at $\pm 45^\circ$ angle and continuing transverse to the tensile load.

According to the obtained UTS values, it is clear that interlayer bonding strength is lower than the strength of the raster itself, which explains the higher tensile strengths obtained for 0° raster angle.

It is noted by some researchers that the mechanical strength depends on the effective area (area excluding voids) rather than the total cross-sectional area [21]. Porosity in the bonding area could influence fracture paths as well as worsen the mechanical properties and is possibly one of the reasons for the weak bonding strength [12]. Investigation of the bonding strength is another interesting point some current studies focused on because enhancement of the effective bonding area would result in higher mechanical strength [22].

4. Conclusions

Raster angle is one of the key parameters affecting the mechanical properties of FDM printed parts. In this work, the influences of this parameter on UTS, strain at fracture and elastic module were evaluated by using four different filaments: PLA, ABS, STH and power ABS. According to the tensile test results carried out for samples printed at 0°, ±45°, 90° raster angles:

- 0° raster angle exhibited the highest ultimate strength for all filaments and UTS values decreased with increasing raster angle. For 0°, the fracture of the tensile samples occurred perpendicular to the applied load due to the failure of the raster; while for 90°, it was due to the failure of the interlayer bonds rather than raster itself. The fracture paths of 45° raster angled samples exhibited both fracture types.
- Highest fracture strains were obtained at ±45° raster angle for all the filaments.
- Elastic module values were not significantly affected by raster angle. Even though the results from this study and the reported values from the suppliers were in agreement for UTS and strain at fracture, inconsistency was noted for elastic module values.
- PLA was found to have the optimum values if both UTS and fracture strain values are considered.
- Surface roughness values were lowest when the measurement direction was parallel to raster direction, dropping below 1 µm; but rose up to 7 µm when the angle between was perpendicular or ±45°. STH exhibited the highest overall values for roughness, while ABS and power ABS showed the lowest.

Acknowledgments

The author acknowledges Volkan M. Küçükakarsu and İbrahim E. Tekin for producing the tensile test samples and Tübitak (The Scientific and Technological Research Council of Turkey) 2209-A grant for financial support.

Nomenclature

FDM	: Fused deposition modelling
UTS	: Ultimate tensile strength
ABS	: Acrylonitrile butadiene styrene
PLA	: Polylactic acid
PC	: Polycarbonate
PA	: Poliamide

References

- [1] ASTM F2792-12a, *Standard Terminology for Additive Manufacturing Technologies*, ASTM International, West Conshohocken, PA, United States (2012).
- [2] D. Shilo, O. Emodi, O. Blanc, D. Noy and A. Rachmiel, Printing the future-updates in 3D printing for surgical applications, *Rambam Maimonides Medical Journal*, 9 (3) (2018) 1-12.
- [3] S. Ford and T. Minshall, Invited review article: where and how 3D printing is used in teaching and education, *Additive Manufacturing*, 25 (2019) 131-150.
- [4] A. Lanzotti, M. Martorelli, S. Maietta, S. Gerbino, F. Penta and A. Gloria, A comparison between mechanical properties of specimens 3D printed with virgin and recycled PLA, *Procedia CIRP*, 79 (2019) 143-146.
- [5] X. G. Zhao, K. Hwang, D. Lee, T. Kim and N. Kim, Enhanced mechanical properties of self-polymerized polydopamine-coated recycled PLA filament used in 3D printing, *Applied Surface Science*, 441 (2019) 381-387.
- [6] D. Amin, N. Nguyen, S. M. Roser and S. Abramowicz, 3D printing of face shields during COVID-19 pandemic: a technical note, *Journal of Oral and Maxillofacial Surgery*, 78 (8) (2020) 1275-1278.
- [7] D. Popescu, A. Zapciu, C. Amza, F. Baciuc and R. Marinescu, FDM process parameters influence over the mechanical properties of polymer specimens: a review, *Polymer Testing*, 69 (2018) 157-166.
- [8] J. R. C. Dizon, A. H. Espera, Q. Chena and R. C. Advincula, Mechanical characterization of 3D-printed polymers, *Additive Manufacturing*, 20 (2018) 44-67.
- [9] M. Kumar, R. Ramakrishnan and A. Omarbekova, 3D printed polycarbonate reinforced acrylonitrile-butadiene-styrene composites: composition effects on mechanical properties, microstructure and void formation study, *Journal of Mechanical Science and Technology*, 33 (11) (2019) 5219-5226.
- [10] ASTM D638-14, *Standard Test Method for Tensile Properties of Plastics*, ASTM International, West Conshohocken, PA, United States (2014).
- [11] ISO 527-1:2019, *Plastics - Determination of Tensile Properties*, International Organization for Standardization, Geneva, Switzerland (2019).
- [12] O. S. Es-Said, J. Foyos, R. Noorani, M. Mendelson, R. Marloth and B. A. Pregger, Effect of layer orientation on mechanical properties of rapid prototyped samples, *Materials and Manufacturing Processes*, 15 (1) (2000) 107-122.
- [13] A. Lanzotti, M. Grasso, G. Staiano and M. Martorelli, The impact of process parameters on mechanical properties of parts fabricated in PLA with an open-source 3-D printer, *Rapid Prototyping Journal*, 21 (5) (2015) 604-617.
- [14] T. Letcher and M. Waytashek, Material property testing of 3D printed specimen in PLA on an entry level 3D printer, *Proc. of the ASME 2014, International Mechanical Engineering Congress Exposition IMECE2014*, Montreal, Quebec, Canada (2014) 1-8.
- [15] T. Lechter, B. Rankouhi and S. Javadpour, Experimental study of mechanical properties of additively manufactured ABS plastic as a function of layer parameters, *Proc. of the ASME 2015, International Mechanical Engineering Congress and Exposition, 2A: Advanced Manufacturing*, Houston, Texas, USA (2015) 1-8.
- [16] I. Durgun and R. Ertan, Experimental investigation of FDM process for improvement of mechanical properties and produc-

- tion cost, *Rapid Prototyping Journal*, 20 (3) (2014) 228-235.
- [17] R. Hernandez, D. Slaughter, D. Whaley, J. Tate and B. Asiabpour, Analysing the tensile, compressive, and flexural properties of 3D printed ABS P430 plastic based on printing orientation using fused deposition modelling, *Proc. of the 26th Annual International Solid Freeform Fabrication Symposium-An Additive Manufacturing Conference*, Austin, Texas, USA (2016) 939-950.
- [18] *Ultimaker ABS TDS*, <https://support.ultimaker.com/hc/en-us/articles/360012759139-Ultimaker-ABS-TDS>, Ultimaker B.V., Utrecht, Netherlands (2020).
- [19] *Ultimaker PLA TDS*, <https://support.ultimaker.com/hc/en-us/articles/360011962720-Ultimaker-PLA-TDS>, Ultimaker B.V., Utrecht, Netherlands (2020).
- [20] *ABG Filament STH TDS*, <http://www.abgfilament.com/assets/images/STH.pdf>, ABG Enterprise, Ankara, Turkey (2020).
- [21] S. Mahmood, A. J. Qureshi, K. L. Goh and D. Talamona, Tensile strength of partially filled FFF printed parts: experimental results, *Rapid Prototyping Journal*, 23 (2017) 122-128.
- [22] T. Marchment, J. Sanjayan and M. Xia, Method of enhancing interlayer bond strength in construction scale 3D printing with mortar by effective bond area amplification, *Materials and Design*, 169 (2019) 107684.



Betül Gülçimen Çakan, born in 1983, received her B.Sc., M.Sc. and Ph.D. degrees in Mechanical Engineering from Bursa Uludağ University in Bursa, Turkey, in 2005, 2008 and 2013, respectively. She worked as a visiting scientist at Institute for Energy at the Joint Research Centre in the Netherlands in 2010 and 2012. Her research areas are mechanics of materials, materials testing, fracture mechanics, creep mechanics, biomechanics and computational modeling of material behaviors. Currently, she is an Assistant Professor in the Mechanical Engineering Department at Bursa Uludağ University, Turkey.